Measurement of differential cross sections for processes $\gamma d \rightarrow pn$, $\pi^0 d$, and pX in the energy range of dibaryon resonances

K. Baba, I. Endo, H. Fukuma,* K. Inoue,† T. Kawamoto,‡ T. Ohsugi, Y. Sumi, T. Takeshita,‡ S. Uehara, and Y. Yano*

Department of Physics, Hiroshima University, Hiroshima 730, Japan

T. Maki

University of Occupational and Environmental Health, Kitakyushu 807, Japan

(Received 9 February 1983)

The differential cross section for the reactions $\gamma d \rightarrow pn$, $\gamma d \rightarrow \pi^0 d$, and $\gamma d \rightarrow pX$ has been measured by using a tagged photon beam in the energy range of dibaryon resonances. The most characteristic feature of the data for $\gamma d \rightarrow pn$ is a forward nonpeaking angular distribution. This behavior is in complete disagreement with the existing predictions which take into account the dibaryon resonances. A phenomenological analysis is made by slightly modifying the model of the Tokyo group, but no satisfactory result is obtained. The data for $\gamma d \rightarrow \pi^0 d$ at large angles show that the differential cross section decreases exponentially as a function of pion angle. A comparison is made with a Glauber model calculation. The result seems to be rather in favor of the existence of dibaryon resonances, but a clear conclusion is not possible because of a lack of more accurate data. In the process $\gamma d \rightarrow pX$, a broad peak due to quasifree pion production is observed, but the limitation of experimental sensitivity does not allow us to have a definite conclusion for the dibaryon resonance of mass 2.23 GeV conjectured by the Saclay group.

[NUCLEAR REACTIONS $^2H(\gamma,p)$, (γ,π^0), $(\gamma,p)X$, $E=180-600$ MeV; measured $\sigma(E,\theta)$; tagged photons. Dibaryon resonance effect.]

I. INTRODUCTION

The dibaryon resonance (DB) was first claimed to be observed in polarized proton experiments at ANL.[1] Unexpectedly striking structures have been observed in cross section differences as well as in various spin parameters. The structures have been ascribed to the effect of DB's by several authors.[2] There have also been predicted theoretically a lot of DB's in a mass range between 2 and 3 GeV. Among them only the $^3F_3$ state has been widely accepted, but no definite conclusion is obtained at present.

On the other hand, a large polarization for protons in the process

$$\gamma + d \rightarrow p + n \quad (1)$$

has been found and a couple of DB's have been introduced to account for the behavior of the polarization by the Tokyo group.[3] This group calculated the contributions from the three graphs in Fig. 1. With the first two the resulting polarization is small and does not depend so largely on the photon energy as the experiment shows. This is the reason why they had to introduce the third diagram. The two DB's in question have masses of 2.26 and 2.38 GeV, respectively.

One of the other sources of information on DB's in the photodeuteron reactions is

$$\gamma + d \rightarrow \pi^0 + d \ , \quad (2)$$

particularly because the πd channel is evidenced to be affected rather strongly by the existence of DB's.[4] In these photodeuteron processes, however, the confirmation or disproof of the existence of DB's is not so straightforward because the existing data are too poor to determine the related invariant amplitudes—whose number is very large owing to the spin complexity. In fact, even for the differential cross section (DCS) of (1), detailed behavior has not been clarified in either the forward and backward regions, where differences among various predictions become large.

Argan *et al.*[5] reported a rapid variation of DCS for the following reaction:

$$\gamma + d \rightarrow p + X \ , \quad (3)$$

around a photon energy of 390 MeV. Comparing their data with a calculated quasifree cross section,[6] they found a bump which might be due to a DB with a mass of 2.23 GeV.

We present here new data of DCS for the processes (1) to (3). The main concern is the excitation function for (1) at four c.m. angles 15°, 30°, 45°, and 72°, for which a preliminary result has been reported in Ref. 7. For the process (2), the DCS was measured at three c.m. angles 117°, 134°, and 153° of pions, for only limited values of k. Finally, the inclusive cross section for (3) is measured at a

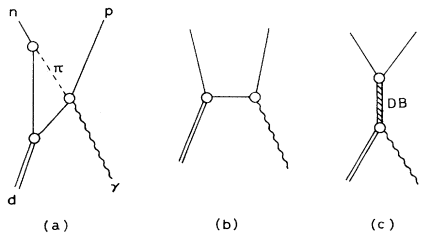

FIG. 1. Feynman diagrams for $\gamma d \rightarrow pn$: (a) One-pion-reabsorption diagram, (b) nucleon-pole diagram, and (c) dibaryon-resonance exchange diagram.

proton lab angle 30°±5° for several fixed values of proton momentum.

II. EXPERIMENTAL METHOD

A. Tagged photons and the liquid deuterium target

The experimental layout is shown in Fig. 2. The electron beam extracted from the 1.3 GeV electron synchrotron at the Institute for Nuclear Study (INS), University of Tokyo, was led to a radiator of aluminum stripping (1.5 mm thick and 100 mm wide). Bremsstrahlung photons produced at the radiator were, after being collimated by a lead collimator, incident upon a liquid deuterium target, while charged contamination was swept out by a magnet.

Recoil electrons from the radiator were deflected by an analyzer magnet and detected by two sets of hodoscopes consisting, respectively, of 24 and 6 pieces of scintillation counter. A coincidence signal between these hodoscopes defined a recoil electron and determined its momentum (namely, its energy E). The energy k of a photon corresponding to the recoil electron was then given by

$$k = E_0 - E \ , \tag{4}$$

where E_0 is the primary energy of the electron. The geometrical setting of the first hodoscope and the field strength of the analyzer magnet were chosen so as to give the same energy acceptance (10 MeV) for each piece of the hodoscope counter. The unscattered electrons were monitored by a scintillation counter (beam spill monitor) and a thin-walled ionization chamber.[8]

The value of k was carefully calibrated with magnetic pair spectrometry. The resulting energy resolution was found to be ±7 MeV, which included uncertainties from finite sizes of the counters, from the primary electron beam, and from the photon beam. The range of k covered by the present tagged photon system was from E_0-125 to E_0-365 MeV for a given value of E_0. The beam intensity was typically 1×10^4 photons/s×(10 MeV). This relatively low intensity was indispensable to avoiding an event in which two or more tagging counters hit within a resolving time of the system, and also to reducing the triggering rate of the hadron spectrometer generated by a photon whose energy was outside the correct range of k; otherwise, we would have had a non-negligible amount of events triggered by a photon with undetermined or incorrect value of k.

The target was liquid deuterium contained in a cylindrical vessel of Mylar. The target length was 198 mm with uncertainties of +0.5% and −2.0%, while the diameter was 50 mm. Possible fluctuation of target density was estimated to be ±0.5% at most.

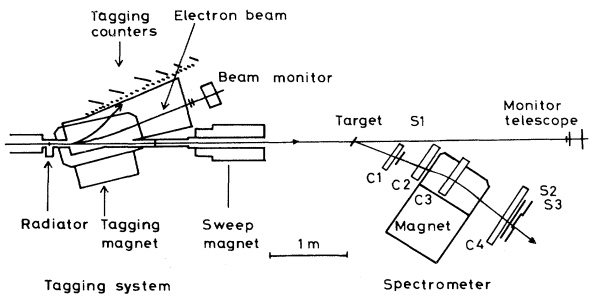

FIG. 2. Plan view of the experimental layout.

B. Hadron spectrometer

Charged particles emerging from the target were detected by the hadron spectrometer consisting of a large-gap analyzer magnet, four sets of multiwire proportional chambers (MWPC's), C1, C2, C3, and C4, and three sets of scintillation counters, $S1$, $S2$, and $S3$. The analyzer magnet was a C-type one with an aperture of 55×50 cm^2, the resulting lab solid angle being typically 30 msr. The field map of the magnet was made by measuring the field strength on 5000 mesh points by Hall probes. In this experiment, charged particles with their momenta above 200 MeV/c were able to be analyzed by a single setting of the magnet.

The trigger system consisted of $S1$, $S2$, and $S3$, where $S2$ and $S3$ were divided into two and three segments, respectively. With a path length of 1.8 m between $S1$ and $S2$, a time of flight (TOF) was measured to determine a particle velocity. Triggered by this system, MWPC's $C1$, $C2$, $C3$, and $C4$ were used to measure a particle trajectory. Each of the chambers had two signal planes which were perpendicular to each other. The largest one $C4$ was of the cathode-readout type.

The above detectors were mounted together on the magnet body and the whole system of the hadron spectrometer was rotatable around the target center. The kinematical conditions under which the present experiment was carried out are summarized in Table I.

C. Trigger logic and data acquisition

A tagged photon signal TAG was defined by a coincidence between any one of 24 counters of the first hodoscope and the corresponding one of the 6 counters of the backing hodoscope, while a particle detected by the hadron spectrometer was defined by a triple coincidence $S123=S1\cdot S2\cdot S3$. Thus an event trigger EV was given by

$$\mathrm{EV}=\mathrm{TAG}\cdot S123 \ .$$

With the present data acquisition system, data consisting of an event included the following kinds of information: (i) hit patterns of the photon tagging hodoscopes and of the trigger counters; (ii) all signals from MWPC's; (iii) TOF signals between $S1$ and $S2$, and $S1$ and TAG; and

TABLE I. Kinematical conditions in the present experiment.

Process	Detected particle	Angle	Range of k (MeV)	Step of k (MeV)
		15°	270—500	
		30°	180—600	
$\gamma d\rightarrow pn$	p	42°	370—600	20
		72°	370—600	
		117°	520—600	
$\gamma d\rightarrow \pi^0 d$	d	134°	440—600	40
		153°	380—500	
$\gamma d\rightarrow px$	p	30° ±5° (in lab system)	320—600	10

(iv) the pulse height of the counter signals. All these data were read out and stored temporarily by a minicomputer. For every 20 events, the minicomputer transferred the stored data to a central computer, where an on-line analysis was made and all the data and results of the analysis were written onto a magnetic tape. The data-taking process was monitored in two ways; one was by the central computer which histogrammed a wire distribution for each of the MWPC's, TOF's, and pulse heights for trigger counters, etc., and another by a microcomputer which displayed the latest data of various kinds on a cathode-ray tube according to a request of an operator of the computer.

III. DATA REDUCTION

A. Beam normalization

The number of incident photons could have been obtained by simply counting the signal TAG. However, there was some part of the signals which did not associate a correctly tagged photon. For example, a certain small fraction of primary electrons could hit the beam pipe, or the residual gases, followed by an electromagnetic shower. These low-energy shower particles could hit the tagging hodoscopes, giving an incorrect TAG signal. In order to estimate a rate of such incorrect TAG's, we measured the number of tagged photons using a lead-glass Cherenkov counter of 11 radiation lengths. In the beginning of each experimental setting, the Cherenkov counter was placed just upstream from the target and the following rate (referred to as tagging efficiency η) was measured:

$$\eta = \mathrm{TAG}\cdot C/\mathrm{TAG} \ ,$$

where C denotes the Cherenkov signal. The result of measurements showed that η depended very weakly on k, being between 0.82 and 0.93. The number of incident photons given by TAG was corrected by this factor.

B. Track reconstruction

The central problem of the data reduction was the determination of particle trajectory. The coordinate system was defined as follows: The central orbit in the spectrometer at each momentum setting was taken as the z axis, while the x and y axes were in the horizontal and vertical planes, respectively. Since a projection of a particle trajectory on the yz plane should be an almost straight line, a combination of y coordinates of MWPC's which gave the best fit to a straight line was picked up from an ensemble of events for which three or more MWPC's were fired. Then, using MWPC coordinates, we calculated the gradients x' and y' with respect to the z coordinate for a trajectory incoming to the magnet.

Next, we assumed a certain value of particle momentum p_{lab} for a given event. By a Runge-Kutta method, the equations of motion for the particle in the magnetic field were solved successively with the initial values for p_{lab}, x, x', y, and y'. Comparison of the calculated trajectory with the measured one gave an improved value for p_{lab} and three or four iterations of this procedure were sufficient to give a final value for p_{lab}. The resulting trajectory was checked by referring to the corresponding hit pattern of segmented trigger counters. An apparently inconsistent event was rejected.

C. Particle identification and event selection

To identify particles, a two-dimensional scatter plot was made for p_{lab} vs TOF between $S1$ and $S2$. A typical example of the plot is shown in Fig. 3. This figure clearly indicates separate bands corresponding to different kinds of particles. Two boundary lines in Fig. 3 are of the form

$$\mathrm{TOF} = a\sqrt{1+m_i^2/p_{\mathrm{lab}}^2}+b \ , \quad (i=1,2) \ ,$$

where $a = 6.27$ ns and b is a constant adjusting the absolute value of TOF. The constants m_1 and m_2 separate deuterons and pions from protons, respectively. Figure 3 shows that there exists almost no ambiguity of particle identification in this experiment.

Once the particle identification was accomplished, the event selection was performed without particular difficulty. Since we employed tagged photons, two-body kinematics gave a unique correlation between p_{lab} and lab angle in the cases of the processes (1) and (2). In fact, a plot of measured values of p_{lab} showed a clear and unambiguous concentration around the value calculated from kinematics using k and lab angles. Applying appropriate cuts, we could isolate wanted events uniquely. On the other hand, for the process (3), only the particle identification was sufficient to give the data of interest.

D. Background subtraction

Since the event selection was critically based on the determination of p_{lab} and k, errors in determining these quantities yielded unwanted background. The major source of errors in k was due to accidental coincidence between TAG and $S123$. This effect was most serious at lower energies, where, for example, in the process (1), protons coming from multibody reactions generated by a photon with its energy higher than those specified by the tagging hodoscopes could simulate protons in (1). In fact, protons from quasifree pion production processes were so copious that even a small fraction of them could amount to appreciable background.

To estimate the contribution of such an accidental event, we measured the event distribution as a function of time difference Δt between TAG and $S123$. A major part

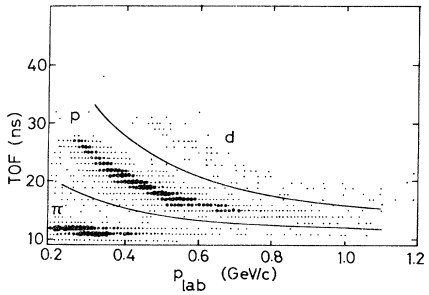

FIG. 3. The scatter plot for events as a function of TOF and p_{lab}. Two curves whose explicit forms are given in the text are used to separate protons from other particles.

of the events had correct timing, while there existed a small but non-negligible contribution even in a region far from correct timing. This background contribution, amounting typically to 20% for protons and 9% for deuterons, did not depend on Δt and therefore was subtracted from the contribution in the region of correct timing.

The background from the target flask and materials other than deuterium was measured in empty-target runs for each kinematical setting. This background was found to be almost constant amounting to 15% of the total events in full-target runs.

E. Geometrical acceptance

The geometrical acceptance of the present detector system was obtained from a Monte Carlo simulation which was carried out for each kinematical setting by taking into account effects of beam size, energy loss, and multiple Coulomb scattering of recoil particles.

F. Corrections

Various corrections had to be applied to the data. The largest correction was due to an inefficiency in track reconstruction which came from either a lack of enough MWPC coordinates or an admixture of too noisy tracks. This inefficiency was estimated in check runs in which an extracted electron beam was directly led into the hadron spectrometer under various setting conditions. The result showed that the inefficiency was almost independent of k, but appreciably dependent on lab angle; it was about 10% for $\gtrsim 20°$, while it increased up to 20% for smaller angles.

Other corrections were the following: (i) the beam normalization correction which consisted of the factor η discussed in Sec. III A, and the beam attenuation effect along the beam path—η was 0.85 at the smallest value of k and 0.90 at the highest, whereas the latter effect was estimated to be less than 1% at any value of k; (ii) loss of outgoing particles mainly due to nuclear interactions with target deuterium; this was estimated from values of total cross section for p-d and d-d scattering. For protons the latter correction was rather small, 2% to 3%, while for deuterons it amounted to 7% to 12%.

The total correction factor resulting from all the above corrections was 1.24 to 1.40. Systematic errors associated with various uncertainties were also estimated: The largest was that for track reconstruction efficiency, which amounted to about 10%, and the second one was that due to ambiguities in various cut values, being typically about 8%, while others were equal to or less than 5%. The total systematic error thus estimated depended slightly on lab angle; for the processes (1) and (3), it was 15% at the smallest angle, while it was 11% at other angles. On the other hand, it was estimated to be 18% to 10% for the process (2).

IV. RESULTS AND DISCUSSION

A. The process $\gamma d \rightarrow pn$

The measured values of DCS's for $\gamma d \rightarrow pn$ are listed in Table II. Errors are statistical only. An overall normalization is accurate to about 15%. The data are also shown in Fig. 4, along with those from other experiments.[9] The consistency among different experiments is generally good except at energies lower than 300 MeV. Around 300 MeV, all the data show a broad peak which is attributed to a $\Delta(1232)$ formation in the intermediate state, but the data themselves scatter rather widely. The data below 300 MeV at 30° from all other experiments are those extrapolated from larger angles. The reason for these discrepancies have, however, not yet been found.

Above 300 MeV, the DCS decreases smoothly as k increases. No remarkable structure is found at any angle. Since the better energy resolution (10 MeV) is attained in the present experiment, a narrow resonance whose width is comparable with this resolution could have been detected, if it existed with an appreciable magnitude. The DB's so far proposed are supposed to have a total width of, say 100 to 300 MeV. Hence, in such a case, if there exist two or more DB's located with an appropriate spacing and contributing constructively to the process, they may smoothly overlap, and as a result, might show no sharp structure in DCS as a function of k. The present data should therefore be interpreted to indicate that there can be no DB which reveals itself as a distinct peak in this energy range.

In Fig. 4, three curves show the prediction of Ikeda *et al.*,[3] who calculated a full amplitude for the diagrams depicted in Fig. 1. The diagram 1(a) represents the one-pion-reabsorption (OPR) process, while 1(b) is the nucleon-pole diagram. These two have been supposed to give background contributions to the present process, whereas 1(c) has been introduced to account for the resonancelike behavior of the polarization data. Values of various parameters included in the calculation were determined so as to fit the data which were available at that time for angles larger than 45° only.

Figure 4 shows that none of the calculated results can reproduce the present cross section data at smaller angles. In Fig. 5, we give the data in the form of an angular distribution. The behavior of the measured DCS at small angles is quite different from that of calculations which con-

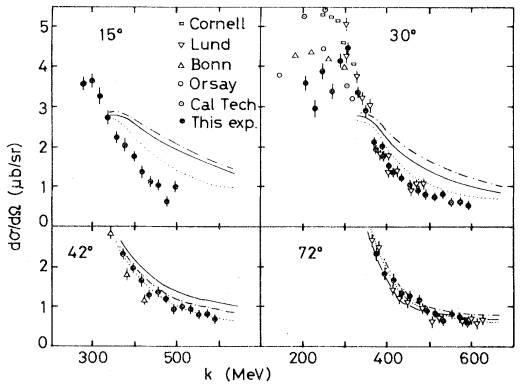

FIG. 4. The DCS for $\gamma d \rightarrow pn$ is shown as a function of k for fixed c.m. angles of protons, 15°, 30°, 42°, and 72°. Three curves are from Ref. 3; the dotted-dashed and the solid curves are two DB's, $3^- + 3^+$, and $3^- + 1^+$, respectively, added to the nonresonance background (NR), while the dotted curve is NR only. In a similar figure in Ref. 7, explanations for the dotted-dashed and solid curves were inverted; here we give correct ones.

TABLE II. Measured values of the DCS for $\gamma d \rightarrow pn$. The errors are statistical only. There is an overall 15% uncertainty in absolute normalization for the data at 15°, while it is about 10% at other angles.

Average photon energy (MeV)	Average c.m. angle (deg)	$d\sigma/d\Omega$ (μb/sr)	Error (μb/sr)	Average photon energy (MeV)	Average c.m. angle (deg)	$d\sigma/d\Omega$ (μb/sr)	Error (μb/sr)
273	15.1	3.60	0.21	513	30.8	0.737	0.062
293	15.0	3.65	0.22	533	31.0	0.827	0.065
313	14.9	3.32	0.24	553	31.2	0.629	0.055
333	14.9	2.74	0.22	573	31.5	0.639	0.055
353	14.8	2.23	0.19	593	31.7	0.558	0.057
373	14.8	2.06	0.18	373	40.3	2.31	0.13
393	14.8	1.77	0.17	393	40.6	1.94	0.13
413	14.8	1.36	0.15	413	41.0	1.67	0.13
433	14.8	1.15	0.15	433	41.4	1.28	0.10
453	14.8	1.04	0.12	453	41.7	1.37	0.099
473	14.8	0.71	0.13	473	42.0	1.22	0.094
493	14.8	0.95	0.12	493	42.3	0.962	0.080
188	24.9	2.74	0.20	513	42.6	0.970	0.080
208	25.5	3.57	0.24	533	42.9	0.941	0.080
228	26.0	2.93	0.25	553	43.2	0.714	0.070
248	26.5	3.92	0.27	573	43.5	0.856	0.080
268	26.9	3.37	0.26	593	43.8	0.684	0.071
288	27.3	4.13	0.24	373	69.7	2.35	0.10
308	27.7	4.49	0.24	393	70.1	1.82	0.19
328	28.1	3.34	0.21	413	70.4	1.70	0.19
348	28.5	2.93	0.19	433	70.8	1.36	0.16
368	28.8	2.13	0.16	453	71.1	1.27	0.14
373	28.9	1.96	0.10	473	71.5	1.19	0.15
393	29.2	1.77	0.10	493	71.8	0.877	0.13
413	29.5	1.37	0.11	513	72.2	0.852	0.12
433	29.8	1.23	0.10	533	72.5	0.659	0.12
453	30.0	1.05	0.083	553	72.9	0.806	0.12
473	30.3	0.933	0.072	573	73.2	0.771	0.13
493	30.5	0.805	0.068	593	73.5	0.596	0.11

tain the diagrams 1(b) and 1(c), while the contribution from only the OPR 1(a) gives an unexpectedly good agreement with the data as shown by the solid curve in Fig. 5. The main reason for this disagreement is due to constructive interference between the diagrams 1(a) and 1(b) at small angles.

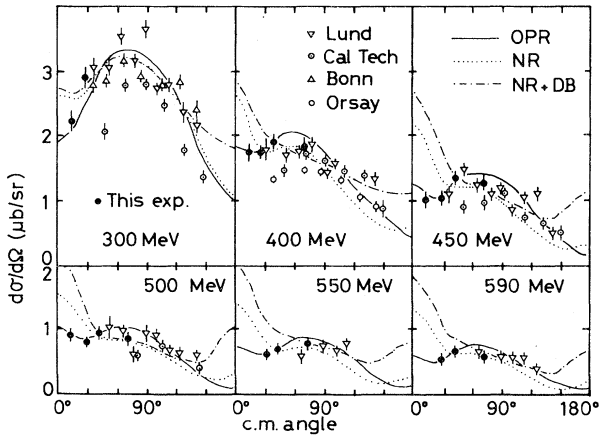

FIG. 5. The DCS for $\gamma d \rightarrow pn$ is shown as a function of c.m. angles of protons at several typical values of k. The solid and the dotted curves represent the OPR contribution and NR (=OPR + nucleon-pole term), respectively, whereas the dotted-dashed curve corresponds to NR$+3^-+3^+$.

A similar situation has been reported also in the pionic processes $\pi^+ d \leftrightarrow pp$,[10] where the difference from the present process is that the incident particle is replaced by a positive pion. This may be due to a kind of double counting; one might consider that when the diagram 1(a) is calculated by means of phenomenological pion production amplitudes, the contribution of 1(b) has already been included in that calculation. Thus we can conclude that the addition of the nucleon-pole diagram in a separate manner should not be justified in this kind of model.

On the other hand, it is clear that only with the OPR amplitude can one not reproduce the observed behavior of polarization and asymmetry parameters. If we note that these spin parameters are very sensitive to small admixtures of resonance amplitude, one of the natural choices for the phenomenological model is to assume that besides the OPR amplitude as a background, there is some contribution from a few DB's conjectured previously, but of small magnitude.

Since the OPR amplitude does not contain any parameters to be adjusted, we have varied all the resonance parameters in the DB amplitude and a phase angle which has been introduced for each DB diagram in 1(c) relative to the diagram 1(a). Starting from values originally given in Ref. 3, we have tried to fit all the existing data of

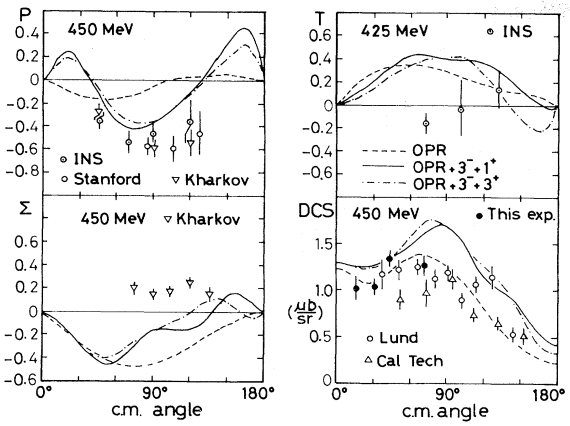

FIG. 6. Typical examples of comparisons of various observables for $\gamma d \rightarrow pn$ with the results of a phenomenological model which is described in the text. The dashed curve represents the OPR contribution as a nonresonance background, while the other two curves, the dotted-dashed and the solid, are OPR$+3^-+3^+$, and OPR$+3^-+1^+$, respectively. The resonance parameters determined in this fit are summarized in Table III.

DCS's,[9] proton polarization P,[3,11] polarized target asymmetry T,[12] and polarized beam asymmetry Σ.[13] Figure 6 shows typical examples of such an attempt at around 450 MeV.

The data are compared with calculated results with a minimum χ^2 for two combinations of spin parity for DB's. The values obtained for the parameters are summarized in Table III.

None of the three curves in Fig. 6 can give any satisfactory fit to the data. This situation is more or less common to all energy points considered. In particular, it is to be noted that within the framework of the present calculation the forward nonpeaking DCS is not compatible with the observed behavior of spin parameters. As a result, we can say that the present data indicate that any set of two DB's conjectured in Ref. 3 is not consistent with experiments.

B. The process $\gamma d \rightarrow \pi^0 d$

The data for $\gamma d \rightarrow \pi^0 d$ are summarized in Table IV. Errors are statistical only. In Fig. 7, the data are compared with those from other experiments.[14] The existing data are confined mainly to forward angles, where the DCS is rather large, while at the present angles, values of the DCS are one order of magnitude or more smaller than those at forward angles. The present data show that the DCS is a fast decreasing function of c.m. angle θ. The angular dependence is well approximated by

$$\frac{d\sigma}{d\Omega} \propto \exp(-\theta/\theta_0) \ ,$$

where θ_0 is a constant which seems to depend on k considerably ($\theta_0=0.44$ at $k=400$ MeV, while $\theta_0=0.73$ at $k=580$ MeV).

In Fig. 8 we show the angular distribution of the present process together with the solid line which expresses the above fit. In this figure are also shown two curves which have been given by Nakamura *et al.*[15] They

TABLE III. Values of resonance parameters obtained in a χ^2 fit using a phenomenological model which is described in the text.

J^P	Mass (GeV)	Width (MeV)	Relative phase (deg)
3^-	2.21	133	−85
3^+	2.23	117	109
3^-	2.24	96	−77
1^+	2.37	651	−11

TABLE IV. Measured values of the DCS for $\gamma d \rightarrow \pi^0 d$. The errors are statistical only; uncertainty in absolute normalization is typically 15%.

Average photon energy (MeV)	Average c.m. angle (deg)	$\frac{d\sigma}{d\Omega}$ (μb/sr)	Error (μb/sr)
538	117	0.116	0.013
578	117	0.070	0.010
459	134	0.174	0.009
497	134	0.100	0.007
540	134	0.080	0.006
578	134	0.046	0.005
400	153	0.157	0.019
439	153	0.074	0.012
478	153	0.067	0.012

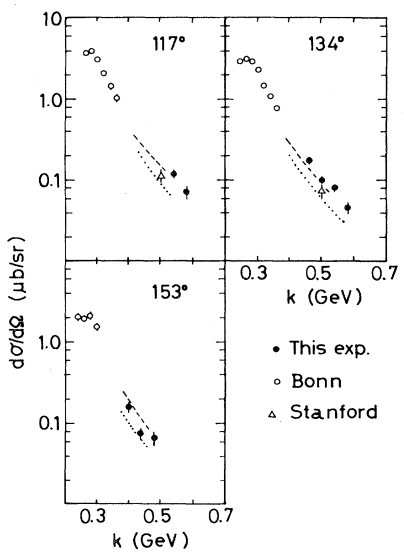

FIG. 7. The DCS for $\gamma d \rightarrow \pi^0 d$ as a function of k at fixed c.m. angles of pions. The data from other experiments (Ref. 14) are also shown for comparison. Also shown are two curves calculated by Nakamura *et al.* (Ref. 15); the dashed curve expresses the contribution from a DB of mass 2.26 GeV and spin-parity of 3^-, added to a nonresonance background which is given by a Glauber model calculation, while the dotted curve is the background contribution only.

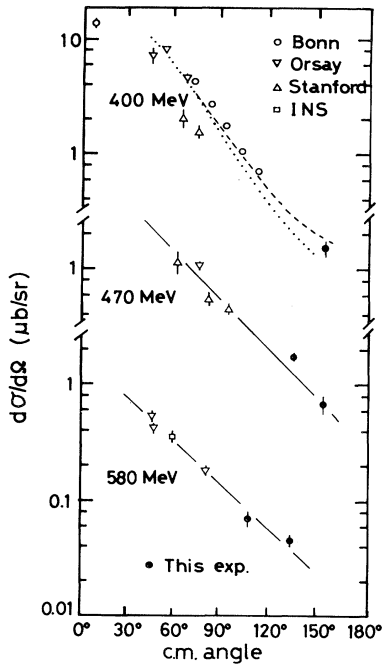

FIG. 8. Some examples of DCS's for $\gamma d \rightarrow pn$ as a function of c.m. angles of pions. The dashed and the dotted curves have the same meaning as in Fig. 7, whereas the solid line gives a fit $\exp(-\theta/\theta_0)$.

assumed that the whole amplitude consisted of a nonresonance background obtained from the single-pion-photoproduction amplitude by means of the Glauber model and a resonance amplitude corresponding to the formation of DB. The dotted curve represents the contribution from the background only, whereas the dashed one gives the contribution of the DB amplitude added to the background. Similar results are also shown in Fig. 7 where curves have the same meaning as in Fig. 8. The resonance parameters taken in this calculation are J^P [mass, width (both in MeV)] $=3^-(2260, 181)$. These results seem to be in favor of the existence of DB, but the number of data points is not enough to make a definite conclusion, even if the reliability of the model is well confirmed.

C. The process $\gamma d \rightarrow pX$

The present data were measured at lab angles $30° \pm 5°$ for proton momenta 520 and 560 MeV/c. Values of double differential cross section $d^2\sigma/d\Omega\, dp$ are listed in Table V. The data are also shown in Fig. 9 as a function of k. The cross section shows a broad peak which corresponds to recoil protons from quasifree pion production[16] and a tail in the higher energy side. The data are well fitted by the following expression, which assumes a Gaussian form for the quasifree peak and a background of a polynomial form up to k^2,

$$\frac{d^2\sigma}{d\Omega\, dp} = a_1 \exp[-(k-a_2)^2/a_3] + a_4 + a_5 k + a_6 k^2 \ ,$$

TABLE V. Measured values of double differential cross section $d^2\sigma/d\Omega\, dp$ for $\gamma d \rightarrow pX$ as a function of k for fixed proton momenta 520 and 560 MeV/c at lab angles $30° \pm 5°$.

	$p=560$ MeV/c		$p=520$ MeV/c	
Average photon energy (MeV)	$d^2\sigma/d\Omega\, dp$ [μb/sr (MeV/c)]	Error [μb/sr (MeV/c)]	$d^2\sigma/d\Omega\, dp$ [μb/sr (MeV/c)]	Error [μb/sr (MeV/c)]
373	0.13	0.03	0.38	0.03
383	0.16	0.05	0.55	0.05
393	0.21	0.05	0.73	0.05
403	0.31	0.05	1.12	0.07
413	0.48	0.06	1.27	0.09
423	0.50	0.05	1.49	0.07
433	0.65	0.07	1.49	0.08
443	0.86	0.07	1.61	0.09
453	1.03	0.07	1.63	0.10
463	1.07	0.07	1.44	0.07
473	1.07	0.06	1.45	0.09
483	1.33	0.07	1.33	0.07
493	1.27	0.07	1.27	0.07
503	1.19	0.07	1.19	0.06
513	0.97	0.06	0.97	0.06
523	1.01	0.06	1.01	0.06
533	0.91	0.06	0.91	0.05
543	0.81	0.07	0.81	0.06
553	0.77	0.05	0.77	0.05
563	0.75	0.06	0.75	0.06
573	0.70	0.05	0.70	0.05
583	0.64	0.05	0.64	0.05
593	0.54	0.05	0.54	0.05

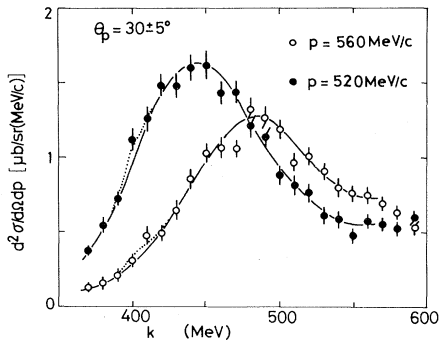

FIG. 9. The double differential cross section $d^2\sigma/dp\,d\Omega$ for the inclusive process $\gamma d \rightarrow pX$, as a function of k for two proton momenta 520 and 560 MeV/c at lab angles 30°±5°. The solid curve represents the fit with a Gaussian form for the peak of quasifree pion production together with a continuous background (a quadratic form in k), and the dotted curve represents the effect of the DB which has been conjectured in Ref. 5.

where a's are to be adjusted to fit the data.

To see if there is an effect of the DB claimed in Ref. 5, which would appear as a structure around $k = 400$ MeV, we add a Breit-Wigner term to the above expression. This term corresponds to the DB of mass 2.23 GeV, the width of 40 MeV, and the integrated cross section of

$$0.4\ \mu\text{b MeV/sr (MeV/}c\text{)} .$$

Again the best fit is searched by varying a's and the result is shown by the dotted curves in Fig. 9. The new fit gives almost the same χ^2 value as that without the DB. The DB effect in question is thus too minute to be clearly confirmed within the present statistical accuracy, which is rather poor at the cost of better energy resolution.

V. CONCLUSION

Using tagged photon beams, we have measured the DCS for the process $\gamma d \rightarrow pn$ at relatively small angles. The data show that the DCS tends to increase slowly as proton angle increases in the forward region. This behavior is in contradiction with the predictions of the Tokyo group, in which the effect of DB's is included to account for the remarkable behavior of proton polarization. The OPR amplitude describes the measured DCS rather well, but a phenomenological model in which the whole amplitude consists of the OPR amplitude as a background and the resonance amplitude with two DB's of possible combinations of their spin-parity ($J^P = 3^- + 3^+$ or $3^- + 1^+$) fails to reproduce simultaneously all the existing data on the process.

We have also measured the DCS for $\gamma d \rightarrow \pi^0 d$ at large angles. The data show a fast decrease of the DCS which is approximately described by an exponentially decreasing function of c.m. pion angle. Comparison with a model in which the DB amplitude is added to the nonresonance background given by the Glauber model calculation indicates that the data are rather in favor of the existence of a DB of mass 2.23 GeV and $J^P = 3^-$, but the number of data points in question is too small for this conclusion to be firm.

The third measurement of the present experiment gives the data for $\gamma d \rightarrow pX$ at proton lab angles 30°±5° as a function of k. The data show a prominent peak due to quasifree pion production. However, the present data are so limited in statistics as the cost of better energy resolution that we have not been able to confirm the effect of DB of mass 2.23 GeV which has been conjectured by the Saclay group.

ACKNOWLEDGMENTS

We wish to thank the synchrotron crew of INS and the staff of the INS computer center for their invaluable support and advice. We are grateful to Professor S. Kaneko and Professor M. Yonezawa for their encouragement. Thanks are also due to Mr. Y. Maeda, Mr. M. Akemoto, and Mr. M. Saito for their assistance in carrying out the present experiment.

*Present address: National Laboratory for High Energy Physics, Tsukuba, Ibaraki 305, Japan.
†Present address: Kobe Steel, Ltd. Kobe 651, Japan.
‡Present address: Laboratory of International Collaboration on Elementary Particle Physics, Faculty of Science, University of Tokyo, Tokyo 113, Japan.

[1]A. Yokosawa, Phys. Rep. 64, 47 (1980); T. Kamae, Nucl. Phys. A374, 25c (1982).
[2]N. Hoshizaki, Prog. Theor. Phys. 60, 1976 (1978); 61, 129 (1979); R. Bhadari *et al.*, Phys. Rev. Lett. 46, 1111 (1981), and references therein.
[3]H. Ikeda *et al.*, Nucl. Phys. B172, 509 (1980); K. Ogawa *et al.*, *ibid.* A340, 451 (1980).
[4]M. Akemoto *et al.* Phys. Rev. Lett. 50, 400 (1983), and references therein.
[5]P. E. Argan *et al.*, Phys. Rev. Lett. 46, 96 (1981).
[6]J. M. Laget, Nucl. Phys. A296, 388 (1978); A335, 267 (1980).
[7]K. Baba *et al.*, Phys. Rev. Lett. 48, 729 (1982).
[8]For the present photon tagging system, see S. Arai *et al.*, Jpn. J. Appl. Phys. 14, 95 (1975).
[9]P. Dougan *et al.*, Z. Phys. A 276, 55 (1976); D. I. Sober *et al.*, Phys. Rev. Lett. 22, 430 (1969); J. Boun *et al.*, Phys. Lett. 26B, 595 (1968); R. Kose *et al.*, Z. Phys. 202, 364 (1967); J. C. Keck *et al.*, Phys. Rev. 101, 360 (1956).
[10]D. O. Riska *et al.*, Phys. Lett. 61B, 41 (1976); T. Yao, Phys. Rev. 134, B454 (1966).
[11]A. S. Bratashevskii *et al.*, Yad. Fiz. 32, 418 (1980) [Sov. J. Nucl. Phys. 32, 216 (1980)].
[12]T. Ishii *et al.*, Phys. Lett. 110B, 441 (1982).
[13]V. G. Gorbenko *et al.*, Nucl. Phys. A381, 330 (1982).
[14]B. Bouquet *et al.*, Nucl. Phys. B79, 45 (1974); G. V. Holtey *et al.*, Z. Phys. 259, 51 (1973); K. Miyake *et al.*, J. Phys. Soc. Jpn. 20, 1749 (1965); J. I. Friedman and H. W. Kendall, Phys. Rev. 129, 2802 (1963); E. F. Ericson and C. Schaerf, Phys. Rev. Lett. 11, 432 (1963).
[15]A. Nakamura, private communication.
[16]K. Baba *et al.*, Nucl. Phys. A306, 292 (1978).